

**FRACTAL MODELING OF THIN-SECTIONS TO DETERMINE
SATURATION EXPONENT FOR VARIOUS WETTING CONDITIONS**

D. Abdassah, Institut Teknologi Bandung, P. Permadi, Institut Teknologi Bandung,
Y. Sumantri, UPN "Veteran", R. Sumantri, Pertamina.

Abstract

A reserve estimate is strongly influenced by the value of saturation exponent adopted. There has been a long standing problem in the petroleum industry as to what value should be used for a given wetting condition. This problem arises due to a remarkable divergence in conclusions derived from laboratory works. A non-laboratory investigation is therefore needed to study the effect of wettability on saturation exponent.

The present study has been directed toward fractal modeling through the use of thin-sectioned core samples in determining the electrical properties. The advantage of this approach is that it is independent of rock-fluid equilibrium problems that commonly influence laboratory measurements. A general equation of electrical resistivity has been developed in this study. Electrical tortuosity, clay content, and rock wettability are incorporated in the equation. The present work employed twenty thin-sections of limestone and sandstones.

Results show that saturation exponents obtained range from 1.6 to 5.0. The exponent consistently increases as the wetting condition is shifted from strongly water-wet toward oil-wet. It is close to 2.0 for clean sandstones at strongly water-wet, supporting the empirical formula of Archie. Results also demonstrate that clay content leads to lower exponent. Increased fractal dimension of pores results in slightly higher exponents for both strongly water-wet and mixed-wet systems, but it reduces the exponent for oil-wet systems. The impact of this study is that knowledge of in-situ reservoir wettability is of high importance in order to correctly use the saturation exponent in evaluating reserve estimates.

I. INTRODUCTION

Quantitative interpretation of electric log data requires knowledge of the so called saturation exponent. The value of the exponent is commonly either assumed to be 2.0 or is derived from laboratory measurements of rock core electrical properties. The Archie equation is then usually used to determine the water saturation.

For many decades, the exponent has been the subject of many laboratory investigations. Researchers (Keller, 1953; Sweeney and Jennings, 1960; Mungan and Moore, 1968; Swanson, 1980; Donaldson and Siddiqui, 1987; Lewis *et al.*, 1988; Cockcroft *et al.*, 1989; Jun-zhi and Lile, 1990) arrived at considerably different quantitative results, particularly for oil-wet cores. Detailed review of this matter has been made by Anderson (1986) and Sondenaa *et al.* (1991).

Little analytical work has been published on the effect of wettability on electrical properties of rocks containing fluids. To handle the complexity of the problems, the present study was directed to applying concepts of fractal analysis to determination of the electrical properties and thus saturation exponent.

II. BACKGROUND

Fractal concepts have been applied to a wide range of research related to porous media at various scales, from microscale (pore level) to megascale (field scale). A detailed review of fractal concepts and applications has been presented by Sahimi and Yortsos (1990). Briefly, a fractal object is an object that has a geometric dimension greater than its topological (Euclidian) dimension. Fractal geometry may describe the irregularity and fragmentation of natural objects and patterns (Mandelbrot, 1982). To characterize a fractal object or set, the fractal dimension D must be determined. A simple method is by "box counting". This is simply done by drawing a mesh of squares of side dimension δ that covers the set. The fractal dimension is determined from the slope of the relation between count and square side dimension.

Pore structures and geometries can be quite complex in nature. The complexity stems from the irregularity of pore wall surfaces. The presence of clays may increase the complexity of pore structures. Therefore, electric tortuosity depends not only on pores connectivity but also on the irregularity of main grain surfaces and volume and distribution of clays within the pores. As pores of a porous medium can be magnified with microscope, identification of fine details can be performed through the microscopic evaluation of thin sections. Ultimately, mathematical analysis coupled with fractal analysis can be used to study electrical properties of porous media.

III. APPROACH OF THE STUDY

Fractal Analysis

Thin sections were prepared from rock core materials. Photos of microscopic thin section images were scanned using a colour scanner. Plots of fractal characteristics were obtained using a mesh of squares. The squares had side dimensions of δ . Plots of count number $N(\delta)$ versus δ were constructed on log-log paper to determine dimensions D_p and D_c for the pores and clays, respectively. At the same time, the porosity ϕ and the fraction of clays V_c were approximated by dividing the number of squares or pixels that capture pores or clays by the total number of pixels covering the image of the whole thin section or the solids part, respectively.

Simulation of the pores containing fluids, oil and water, was performed by assigning a given colour to a given fluid within the pores. The minimum diameter of a non-wetting fluid within each pore was equivalent to the side of one pixel of the mesh generated. The maximum diameter depended on the maximum capillary pressure assumed for the porous media. Furthermore, for strong wetting conditions, the minimum thickness of the wetting fluid bound to pore walls was one pixel. Whereas for mixed wettability cases, the oil was only in contact with pores larger than a certain number of pixels.

For all systems under study, water saturation was varied by replacing some oil pixels with water pixels. By employing a box counting method, fractal dimension of pores containing water at a given saturation can thus be determined. This is of importance as will be described in the next two sections.

Electrical Tortuosity

Tortuosity may represent the path that electric current must take. Assuming that L_a is the length of the path and L is the measurable length of the porous media, then $(L_a/L)^2$ is referred to as tortuosity. As we consider that the flow of electric current might depend upon pores structure and distribution, water saturation, and wetting condition as well, we then suggest that electric tortuosity of a given fluids-saturated porous medium is not unique but is dependent of the fluids saturation and fractal characteristics of the medium.

Mathematical derivation of electrical properties by incorporating fractal characteristics is not easy to solve. To handle this situation, a simplified approach was adopted by assuming that electric tortuosity at water saturation of 100 %, also usually called as hydraulic tortuosity, can be handled by the squared ratio of fractal dimension of single-pore system (D_s) to multi-pore system (D_m) with the same porosity value. This is mathematically written :

$$\tau = \left(\frac{L_a}{L}\right)^2 \cong \left(\frac{D_s}{D_m}\right)^2 \quad (1)$$

Where D_s was found to have relationship with porosity (Sumantri, 1995) :

$$D_s = 2.0061769 \phi^{0.02874553} \quad (2)$$

For future discussion we use D_p for fractal dimension of multi-pore system, instead of D_m . If clays present within the rock is assumed to be electrically conductive, the tortuosity due to clay :

$$\tau_c = \left(\frac{L_c}{L}\right)^2 \cong \left(\frac{D_{sc}}{D_c}\right)^2 \quad (3)$$

Where D_c is fractal dimension of clays and D_{sc} is fractal dimension of single pore with porosity equal to the clay fraction.

Electrical Resistivity of Rocks

Suppose we have a fluids-saturated core sample with area A , length L , porosity ϕ , and water saturation S_w , one may write that the effective area A' for electric current :

$$A' = \phi S_w P_{sw} \left(\frac{L}{L'_a}\right) A \quad (4)$$

Where L'_a is effective length of the path for electric current to take and P_{sw} is probability of electrical conductance, which depends on wetting condition of the sample :

- for strongly water-wet sample,

$$P_{sw} = 1 \quad (5a)$$

- for strongly oil-wet sample,

$$P_{sw} = (S_w)^2 \quad (5b)$$

- for mixed wettability,

$$P_{sw} = S_w(2-S_w) \quad (5c)$$

Now, the true conductivity of the sample with clays present can be written :

$$C_t = \frac{LA'_a}{R_w L'_a A} + \frac{LA_c}{R_c L_c A} \quad (6)$$

where R_w is water resistivity, A_c is the area covered with clays, L_c is effective length of clays, and R_c is clays resistivity.

Substituting Eq. (4) into Eq. (6) and changing the second term of Eq. (6) in terms of clay fraction V_c , one can find :

$$C_t = \frac{\phi S_w P_{sw} R_c L_c^2 + V_c R_w L'_a \left(\frac{L}{L'_a L_c} \right)^2}{R_w R_c} \quad (7)$$

or the true resistivity :

$$R_t = \frac{R_w R_c}{\phi S_w P_{sw} R_c L_c^2 + V_c R_w L'_a \left(\frac{L}{L'_a L_c} \right)^2} \quad (8)$$

For conditions at which $S_w < 100\%$, and taking Eqs. (5) into consideration, Eq. (1) is modified :

$$\tau' = \frac{(L'_a)^2}{P_{sw} L^2} \cong \frac{(D'_s)^2}{P_{sw} (D'_p)^2} \quad (9)$$

where primed parameters are for $S_w < 100\%$.

Substituting Eq. (3) and Eq. (9) into Eq. (8) and applying Eq. (2) to D'_s and D_{sc} by replacing ϕ with $S_w (< 100\%)$ and V_c , respectively, result in a final form :

$$R_t = \frac{4.024746 R_w R_c}{P_{sw} R_c (\phi S_w)^{0.94251} (D'_p)^2 + R_w (V_c)^{0.94251} D_c^2} \quad (10)$$

Similarly, one can easily find for the rock saturated completely with water :

$$R_o = \frac{4.024746 R_w R_c}{R_c \phi^{0.94251} D_p^2 + R_w V_c^{0.94251} D_c^2} \quad (11)$$

Again, D_p and D'_p are fractal dimensions of pores occupied by water at $S_w = 100\%$ and $S_w < 100\%$, respectively.

The resistivity ratio can then be written :

$$\frac{R_o}{R_t} = \frac{P_{sw} R_c (\phi S_w)^{0.94251} (D'_p)^2 + R_w V_c^{0.94251} D_c^2}{R_c \phi^{0.94251} D_p^2 + R_w V_c^{0.94251} D_c^2} \quad (12)$$

Or we can modify Eq. (12) to approach the Archie's empirical form :

$$\frac{R_o}{R_t} = a + b S_w^n \quad (13)$$

Where a = a constant for a given core containing water with R_w

$$= \frac{R_w (V_c)^{0.94251} D_c^2}{R_c \phi^{0.94251} D_p^2 + R_w V_c^{0.94251} D_c^2} \quad (14)$$

b = a coefficient that depends on the pores structure, water distribution, clay content and distribution, and the core wettability

n = saturation exponent.

IV. RESULTS AND DISCUSSION

Rocks Used and Fractal Analysis

Two shaly sandstone cores and two limestone cores were available for this study. Six and four thin-sections for each sandstone core and limestone core sample, respectively, were made. Scanned pictures of typical thin sections representing the type of rocks used are shown in Figure 1 and Figure 2. The method and procedure employed to perform fractal analysis have been described in the section III above. We used a mesh of 400X600 pixels and 16 color mode. All parameters, such as porosity, clay content, fractal dimensions of pores and clay, for each core sample shown in this paper are the arithmetic average values of the respective thin-sections (see Table 1).

Hydraulic or pore tortuosity was also determined employing Eq. (1) for all the thin-sections of each core. The average value is 2.008 for core SS-1, 2.762 for SS-2, 1.598 for LS-1, and 1.563 for LS-2. These values are within the normal range ($1 \leq \tau \leq 3$) as stated by Dullien (1979). For these particular core samples used in the present study, the pore tortuosity of sandstones is higher than that of limestones. Electrical tortuosity, however, can be higher than 3.0 at relatively low water saturation, particularly for mixed and oil wet conditions.

Electrical Properties and Saturation Exponent

In calculating the true resistivity R_t of a given system/thin section, saturation of non-wetting fluid was varied from the size of one pixel to the size equivalent to six pixels. So, we have about six varied water saturation for each core sample, depending on the pore size distribution. Note that not all pores contained non-wetting fluid and the number of non-wetting pixels in each pore depended on its size.

Results for samples SS-1, SS-2, LS-1, and LS-2 at strongly water-wet, mixed wet, and strongly oil-wet conditions are shown in Figures 3 to 6, respectively. In the present study, we used water resistivity $R_w = 0.1$ ohm-m and clay resistivity $R_c = 0.8$ ohm-m, and assumed that rock grains are not conductive. For each core sample, a is constant and was calculated using Eq. (14). At strongly oil-wet conditions, we assumed that clays were also wetted by oil. Also, $a = 0$ for rocks with no clays (see Eq. (14)).

According to Eq. (13), the best-fitting curve drawn on data points of each wetting condition resulted in values of saturation coefficient b and exponent n as shown in Table 2. As inferred from this table, basically for sandstones, the values of a are all close to zero and b close to one at strongly water-wet and mixed wet conditions, but not at strongly oil-wet ones. It is interesting to note that mixed wet sandstone cores containing clays behave like water-wet systems (see also Figures 3 and 4), supporting the experimental results of Swanson's study (1980). Results obtained for limestone cores, as shown in Figures 5 and 6, are somewhat different. These outcomes should be understood because the limestone cores used here do not contain any clays. The trend for all cores studied is, however, the same in that the saturation exponent increases as the wetting condition is shifted from strongly water-wet toward strongly oil-wet condition.

The effect of clay content was studied by assuming $V_c = 0$ and the results are given in Table 3 for sandstone core samples. We found that the values of b for the two cores at either strongly water-wet or mixed-wet condition are about one,

supporting the Archie's empirical formula. The saturation exponent for clean sandstone is again close to 2.0. Whilst, the exponent for mixed wettability remains higher than 2.0. Comparing these with results shown in Table 2, we conclude that the presence of clays reduces the saturation exponent.

To study the effects of pores structure and size distribution on the values of saturation exponent, fractal analysis might be meaningful. In this effort, the clays fraction was not considered ($V_c = 0$) and then the calculated data points were analyzed by implementing the original Archie's empirical formula. The results are shown in Table 4. The saturation exponents for all wetting conditions in general are slightly lower than the previous results interpreted using Eq. (13) as discussed above.

Figure 7 demonstrates a clearer view of the effects of fractal dimension, manifesting pores structure and pores size distribution, on saturation exponent at different wetting conditions. For these particular rock samples, fractal dimension of limestone pores is higher than that of sandstone. This is true because the limestones used have many much larger pores. For the same type of rocks, higher porosity would result in higher fractal dimension. In the present study, Figure 7 suggests that for a given type of rock at strongly water-wet and mixed wet conditions saturation exponent increases with fractal dimension. Oppositely, the exponent is reduced as fractal dimension increases at strongly oil-wet condition.

V. CONCLUSIONS

1. Fractal analysis of thin sections of real porous rocks and mathematical modeling for investigating saturation exponent at various wetting conditions have been conducted.
2. Natural sandstones and limestones have been used in the present study. The values of saturation exponent obtained are quantitatively reliable. The range is from 1.6 to 2.0 for strongly water wet, 1.9 to 2.8 for mixed wet, and 3.4 to 5.0 for strongly oil-wet systems.
3. For the same type of rocks used in this study, there is a trend exhibiting increased saturation exponent for higher fractal dimension at strongly water-wet and mixed wet conditions. It happens inversely for strongly oil-wet systems.
4. The values of saturation exponent for the strongly water-wet and mixed wet clayey sandstones were slightly different but the difference tends to be higher when the clays contained was neglected.

VI. ACKNOWLEDGMENT

This research work is supported by the PERTAMINA Research Grant. The authors express sincere gratitude to the management of PERTAMINA for the permission to publish and present this paper. The authors also express sincere appreciation to Mr. Irwan Kurniawan for his helps during the preparation of the manuscript.

VI. REFERENCES

1. Anderson, W.G., "Wettability Literature Survey-Part 3 : The Effects of Wettability on the Electrical Properties of Porous Media", J. of Petr. Tech., Dec., 1986.

2. Archie, G.E., "The Electrical Resistivity Log as an Aid in Determining Some Reservoir Characteristics", Trans. AIME, 1942.
3. Cockcroft, P.J, Guise, D.R, and Waworuntu, I.D, "The Effect of Wettability on Estimation of Reserves", SPE 19484, the SPE Asia-Pacific Conference, Sydney, Australia, 13-15 September, 1989.
4. Donaldson, E.C., and Siddiqui, T.K., "Relation Between the Archie Saturation Exponent and Wettability", SPE Formation Evaluation, Sept., 1989.
5. Dullien, F.A.L., *Porous Media Fluid Transport and Pore Structure*, Academic Press, Inc., 111 Fifth Avenue, New York, New York 10003, 1979.
6. Jun-Zhi, W. and Lile, O.B., "Hysteresis of the Resistivity Index in Berea Sandstone", *Advances in Core Evaluation*, Gordon and Breach Science Publishers, ISBN 2-88124-766-0, 1990.
7. Keller, G.V., "Effect of Wettability on the Electrical Resistivity of Sand", The Oil and Gas Journal, January 5, 1953.
8. Lewis, M.G., *et al.*, "Wettability and Stress Effect on Saturation and Cementation Exponents, presented at the SPWLA 29th Annual Log Symposium, 1988.
9. Mandelbrot, B.B., *The Fractal Geometry of Nature*, W.H. Freeman & Co., New York, 1982.
10. Mungan, N. and Moore, E.J., "Certain Wettability Effects on Electrical Resistivity in Porous Media," The J. of Canadian Petr. Tech., Jan-Mar., 1968.
11. Sahimi, M. and Yortsos, Y.C., "Application of Fractal Geometry to Porous Media : A Review", paper SPE 20476, SPE Annual Fall Meeting, 1990.
12. Sondena, E. *et al.*, "The Effect of Reservoir Conditions and Wettability on Electrical Resistivity," paper SPE 22991, SPE Asia-Pacific Conference, 1991.
13. Swanson, B.F., "Rationalizing the Influence of Crude Wetting on Reservoir Fluid Flow With Electrical Resistivity Behaviour," J. of Petr. Tech., Aug., 1980.
14. Sweeney, S.S and Jennings, H.Y., "Effect of Wettability on the Electrical Resistivity of Carbonate Rock from a Petroleum Reservoir," J. of Phys. Chemistry, v. 64, May, 1960.

Table - 1 Results of Boxcounting Method

Core Number	Type of Rock	Porosity (fraction)	V_c (fraction)	D_p	D_c
SS-1	Sandstone	0.2526	0.242	1.3619	1.2189
SS-2	Sandstone	0.1853	0.1853	1.1525	1.1132
LS-1	Limestone	0	0	1.5166	0
LS-2	Limestone	0	0	1.542	0

Table-2 Parameters derived for cores used at various wetting conditions

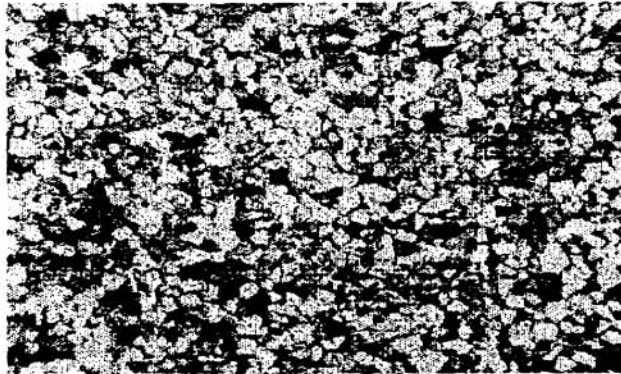
Condition		Core-1	Core-2	Core-3	Core-4
		$D_{pore}=1.3619$ $V_{clay}=0.2420$	$D_{pore}=1.1525$ $V_{clay}=0.1853$	$D_{pore}=1.5166$ $V_{clay}=0$	$D_{pore}=1.5420$ $V_{clay}=0$
Water-wet	a	0.0168	0.0272	0	0
	b	0.9862	0.9965	1.2023	1.0786
	n	1.6074	1.7888	1.8421	1.8799
Mixed-wet	a	0.0168	0.0272	0	0
	b	1.0057	1.0207	1.6081	1.3166
	n	1.8949	2.1687	2.6876	2.7866
Oil-wet	a	0	0	0	0
	b	20.3693	5.1111	2.0682	1.5335
	n	4.9933	4.2087	4.9735	4.1425

Table-3 Parameters derived for sandstone cores assuming $V_c=0$ or clean sand

Condition		Core-1	Core-2
		$D_{pore}=1.3619$	$D_{pore}=1.1525$
Water-wet	a	0	0
	b	1.0102	1.0365
	n	1.9077	1.9652
Mixed-wet	a	0	0
	b	1.0807	1.0772
	n	2.5512	2.4885

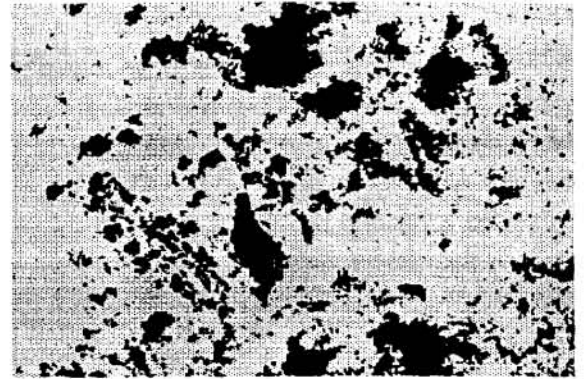
Table - 4 Saturation exponent derived from application of Archie Equation to the calculated data points

Condition	Core1	Core2	Core3	Core4
Water-wet	1.8697	1.6714	1.5897	1.7808
Mixed-wet	2.3307	2.098	2.2411	2.5344
Oil-wet	3.4134	3.8534	3.9574	3.5091



■ pore ■ clay ■ matrix

Figure 1 - A typical thin section of sandstone core sample



■ pore ■ matrix

Figure 2 - A typical thin section of limestone core sample

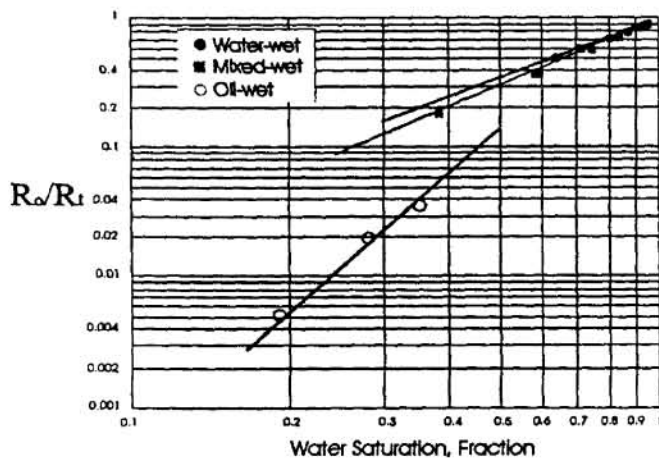


Figure 3 - Resistivity ratio versus water saturation for Core SS-1

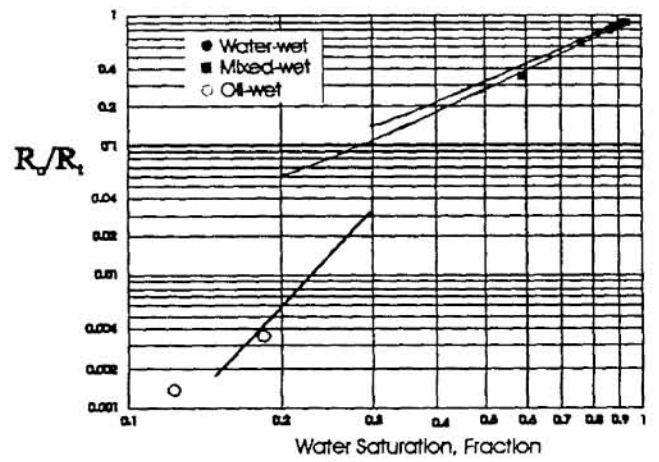


Figure 4 - Resistivity ratio versus water saturation for Core SS-2

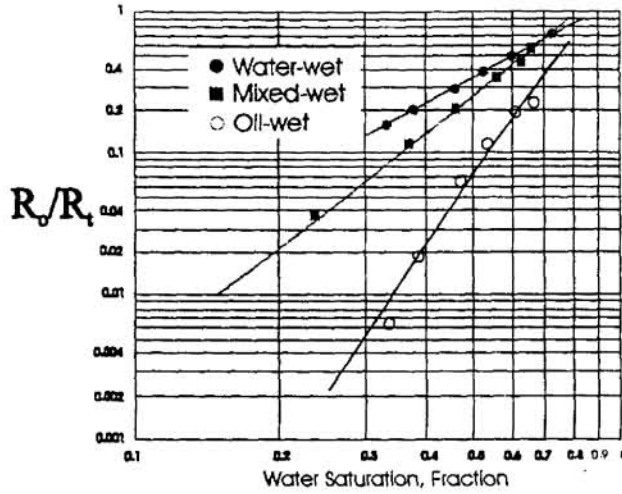


Figure 5 - Resistivity ratio versus water saturation for Core LS-1

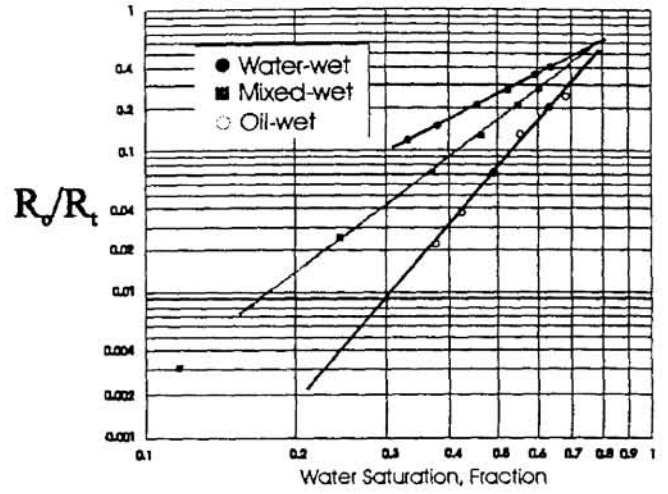


Figure 6 - Resistivity ratio versus water saturation for Core LS-2

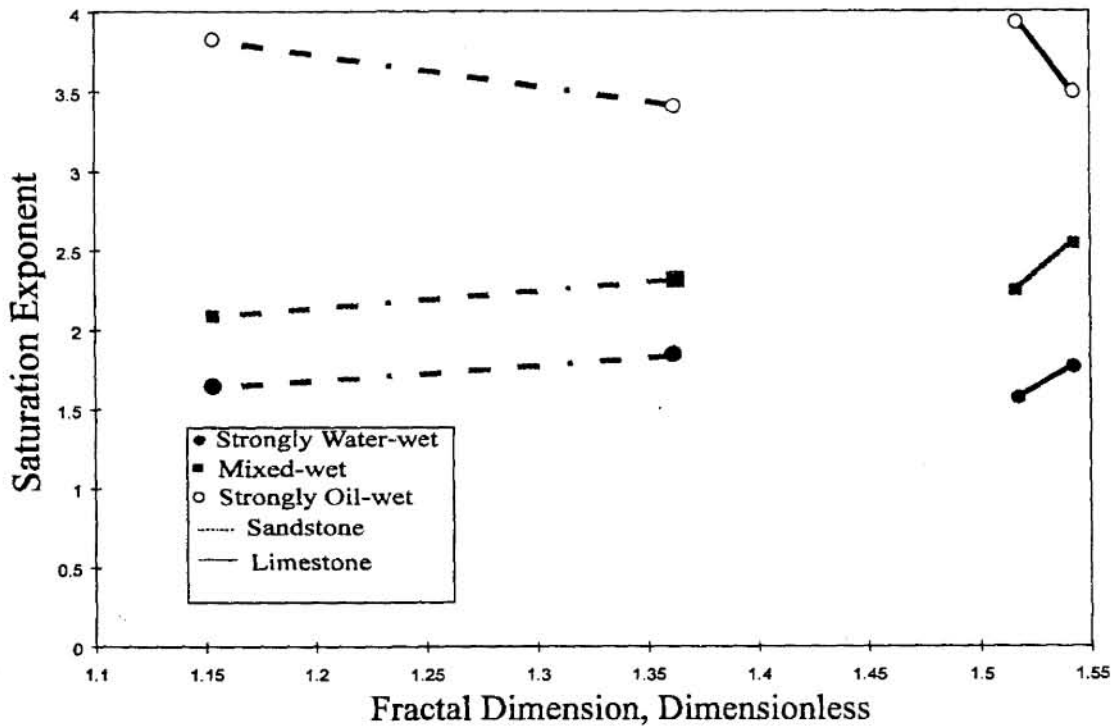


Figure 7 - Relationship between saturation exponent and fractal dimension for various wetting condition.